Statistical and neural network assessment of the climatology of fog and mist at Pula airport in Croatia

Marko Zoldoš*[1,2], Tomislav Džoić*[3], Jadran Jurković[2], Frano Matić[4], Sandra Jambrošić[2], Ivan Ljuština[2], Maja Telišman Prtenjak[5]

[1]Risk Management Division, Erste & Steiermärkische Bank d.d., Rijeka 51000, Croatia (ORCID: 0009-0005-1117-5716)
[2]Aviation Meteorology department, Croatia Control Ltd., Velika Gorica 10410, Croatia
[3]Laboratory of Physical Oceanography, Institute of Oceanography and Fisheries, Split 21000, Croatia
[4]Department of Marine Studies, University of Split, Split 21000, Croatia (ORCID: 0000-0003-0392-4172)
[5]Department of Geophysics, Faculty of Science, University of Zagreb, Zagreb 10000, Croatia (ORCID: 0000-0002-4941-8278)

*_Leading author_: Marko Zoldoš, _correspondence to_: Tomislav Džoić (dzoic@izor.hr)

Abstract. A study was conducted on the climatological characteristics of fog and mist at Pula Airport in the northeastern Adriatic, using statistical and machine learning approaches. The study utilized meteorological data from Pula Airport, along with satellite sea surface temperature (SST) data from two coastal areas west and east of the airport, to gain insights into the influence of sea temperature on fog formation. To identify weather patterns associated with the occurrence of fog and mist, wind and mean sea-level pressure (MSLP) data from the ERA5 reanalysis were analyzed using Growing Neural Gas (GNG), a machine learning method. A notable finding was a declining trend in the frequency of fog and mist at the airport, which can be linked to the results of the GNG analysis of the ERA5 data. This analysis showed a decrease in synoptic patterns favorable for fog and mist. Fog occurs mainly between October and March and is primarily associated with weak westerly and northwesterly winds. Additionally, fog is more likely to occur when the sea surface temperature is higher than the air temperature. Mist has similar characteristics to fog, although it is more likely to occur with easterly winds.

1 Introduction

According to the World Meteorological Organization (WMO), fog is the suspension of very small water droplets or ice crystals in the atmosphere, reducing visibility on the Earth's surface to less than 1 km (WMO, 1966). The formation of these water droplets and ice crystals is influenced by factors such as cooling, increased humidity, and the mixing of air masses with different temperatures (Gultepe et al., 2007). Mist, a related phenomenon, occurs when horizontal visibility at the surface is between 1 and 10 km, with aviation meteorology specifically defining mist as conditions where visibility is between 1 and 5 km. Fog is a unique atmospheric phenomenon confined to the atmospheric boundary layer (ABL), the lowest part of the atmosphere, and its characteristics are influenced by the Earth's surface. The formation and dissipation of fog are impacted by synoptic and mesoscale conditions, as well as surface features such as moisture sources (e.g., oceans, lakes, rivers), vegetation, orography, urban areas, and sea currents.

This study examines fog occurrence over an extended period at Pula Airport, located in the coastal region of Croatia in the northeastern Adriatic (Figure 1). The Adriatic Sea is a large semi-enclosed sea separating the Apennine Peninsula from the Balkans. It is the northernmost arm of the Mediterranean Sea, extending from the Strait of Otranto (where it connects to the Ionian Sea and the rest of the Mediterranean) to the northwest, toward the Po Valley and the Istria Peninsula. This region frequently experiences marine fog due to synoptic-scale effects that can trigger subsidence within the boundary layer, which causes stratus clouds to descend to the surface. Similar marine fog events have been studied in the northwestern Pacific and Atlantic Oceans (e.g., Koračin et al., 2001; Koračin and Dorman, 2017). In the Adriatic, fog typically occurs between September and May, often disrupting sea transport and port operations (Popović et al., 2014). Fog also significantly affects air traffic at airports, where it can cause significant flight delays due to poor visibility and low cloud ceilings. These delays result in substantial financial losses for airlines, underscoring the need for accurate fog forecasting. For example, dense fog at New Delhi Airport in India caused losses of approximately 3.9 million U.S. dollars between 2011 and 2016 (Kulkarni et al., 2019). Improved fog forecasting could mitigate such losses, as illustrated by Allan (2001), who estimated that better forecasts for low-visibility events at three New York City airports could save up to $240,000 per event.

These factors highlight the critical role of fog research in advancing forecasting capabilities. Despite its importance, the study of fog remains an area of atmospheric science where our understanding is limited, both over land (Gultepe et al., 2007) and ocean (Koračin and Dorman, 2017). Fog formation involves a complex interaction of processes ranging from synoptic to microscale levels. The typical size of fog condensation nuclei is around 0.1 μm (10^{-5} cm), while the synoptic-scale processes that contribute to fog development occur on a scale of 10^{8} cm or more, making the ratio of interacting length scales about 10^{13}. Fully understanding fog formation involves various elements, including large-scale synoptics (Belo-Pereira and Santos, 2016), characteristics of the surface and radiation exchange (Duynkerke, 1991), microphysics (Gultepe and Milbrandt, 2007; Wang et al., 2019), climatology (Stolaki et al., 2009; Veljović et al., 2015), relationships with turbulence intensity (Ju et al., 2020), presence of aerosol (Oztaner and Yilmaz, 2013), and more. The complicated interplay of meteorological parameters that determine whether fog forms or not poses a substantial challenge for accurate fog forecasting (Bergot and Koračin, 2021). In addition to local factors

influencing fog and mist formation, the impact of global warming and climate change cannot be overlooked. These global phenomena have been linked to a reduction in the number of days with fog and mist (Kawai et al., 2016; Klemm and Lin, 2016). Considering that fog occurrence in the eastern Adriatic has been studied infrequently, with the most recent research conducted over 50 years ago (Stipaničić, 1972), there is a need for updated insights.

This study analyzes the climatological characteristics of fog at Pula Airport, Croatia, with a focus on understanding the general patterns of fog initiation and dissipation. The primary objective is to provide detailed statistical analyses to help understand the local and dynamic processes leading to fog development. A secondary objective is to assess the influence of sea surface temperature (SST) in the vicinity of the study area on the frequency and intensity of advective fog. SST has been shown to significantly impact the accuracy of numerical weather prediction (NWP) models (Huang et al., 2022). To achieve these goals, the Growing Neural Gas Network (GNG), an unsupervised machine learning algorithm within artificial neural networks (Martinetz and Schulten, 1991), was applied. This method classifies synoptic conditions that prevail before and during the occurrence of fog at Pula into distinct weather patterns, and identifies those that favor fog development. The results of this research could aid local forecasters in improving fog prediction by accounting for specific terrain and coastline features, as well as synoptic and local influences (particularly SST), thereby closing a gap in scientific knowledge about fog characteristics in this part of the Mediterranean.

2 Location, data and methods

2.1 Location

Pula Airport, located approximately 6 km ENE of the coastal city of Pula in western Croatia (Figure 1b), serves as the region's international airport. Its geographical coordinates are 44°53'37" N and 13°55'20" E, with an elevation of 84 meters above mean sea level (AMSL). In 2023, the airport served 413,439 passengers, ranking as the fifth busiest airport in Croatia by passenger traffic (source: https://podaci.dzs.hr/2023/en/58556). The airport is situated at the southern tip of the Istrian Peninsula—the largest peninsula in the Adriatic Sea—positioned between the Gulf of Trieste to the northwest and the Kvarner Gulf to the east. The climate of Istria is influenced by Alpine and Dinaric Alps mountain ranges and the Mediterranean Sea. Winters in Istria are typically mild and wet, while summers are hot and humid. The interior of Istria experiences a more continental climate, while the coastal area is significantly influenced by the Adriatic Sea. Recent research has analyzed bioclimatic parameters, highlighting these climatic boundaries across the peninsula (e.g., Omazić et al., 2020).

Two weather patterns are primarily associated with fog in Pula. The first involves a westerly to northwesterly flow that advects moist air under anticyclonic conditions. In these cases, advection can occur over a broad geographical area. Fog is often advected from the Po Valley in northern Italy, where it is a frequent phenomenon during the fall-winter season (Mariani, 2009), across the northern Adriatic to the Istrian coast. Under such conditions, fog can persist for days across the affected region (Bendix, 1994). For example, Linate Airport in Milan, Italy, historically

experienced the highest number of annual closures due to fog among European airports (Mariani, 2009). While advective fog is less common in the northwestern Adriatic, it still frequently occurs on the western coast of Istria (Tešić and Brozinčević, 1974), which is climatologically the foggiest area of the eastern Adriatic (Stipaničić, 1972). The second weather pattern associated with fog in Pula involves an easterly to southeasterly flow during a weakening anticyclone, often advecting moist air from the southeast. These patterns are linked to the broader atmospheric circulation over the Adriatic Sea, which is shaped by four dominant wind regimes. The northeasterly bora and the southeasterly sirocco winds, both common in the colder months, are influenced by regional synoptic systems. In contrast, during warmer months, sea/land breezes and, to a lesser extent, the Etesian wind, become more prominent. The wind regime strongly influences changes in wind direction at Pula Airport (e.g., Pandžić and Likso, 2005; Prtenjak and Grisogono, 2007; Prtenjak et al., 2010; Belušić et al., 2018).

The terrain surrounding the airport is predominantly flat, covered with grassland and small forested areas. There are no significant hills or mountains nearby that would notably influence the local weather or climate. The central part of the airport, along with its southern surroundings, lies within a very shallow basin, which is prone to nighttime inversions during calm wind conditions and clear skies (as reported by local forecasters). The proximity of the sea exerts a substantial influence on the airport's weather. Pula Bay is located 6 km to the west-southwest, while the open waters of the northern Adriatic Sea are just 10 km away. To the east, the open sea is 7 km away, with the small Bay of Kavran situated just 5 km from Pula Airport. These geographical factors contribute to the significant marine influence on the weather at Pula Airport, even though the airport itself is not directly on the coast.

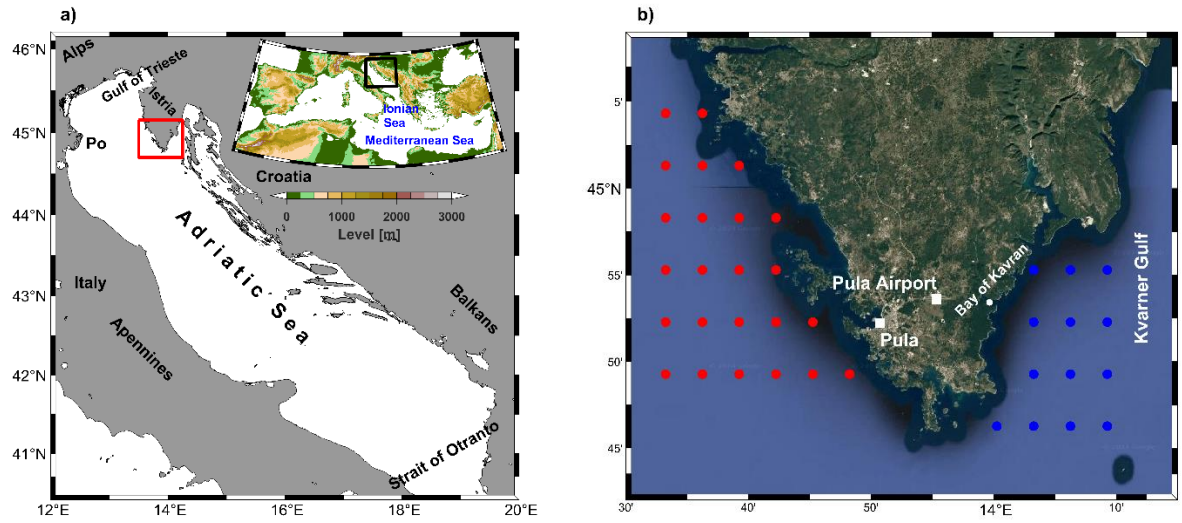

Figure 1. a) Map of the bathymetry of the Adriatic Sea, with the black square marking the Adriatic Sea area. The red rectangle on the map marks the immediate surroundings of Pula Airport (b) (© Google Maps 2024). The important localities are marked with white squares, while blue and red dots mark the eastern and western grid points from which the satellite SST values were extracted. The wider area of the Mediterranean Sea corresponds to the area of the ERA5 reanalysis.

2.2 Data and methods

The dataset used for this study includes half-hourly METAR reports and three-hourly SYNOP reports from the meteorological station at Pula Airport. METAR (METeorological Aerodrome Report) is a coded report describing weather conditions at the airport in a manner standardized for aviation. SYNOP (Surface Synoptic Observations) is a coded report describing weather conditions at a meteorological station. An airport meteorological station sends both SYNOP and METAR reports. The meteorological variables considered are wind speed and direction, temperature at 2 meters above ground, dew point temperature, relative humidity, surface pressure, cloud cover, and horizontal visibility. These variables are reported by both station observers and automatic instruments. The dataset spans a 20-year period from January 1, 2001, to December 31, 2020, with all measurements recorded at the airport's meteorological station. Runway 27, the primary operational runway, is equipped for Category I operations. This allows for takeoff and landing under low visibility conditions with a Runway Visual Range (RVR) of up to 550 meters or a ceiling height of 200 feet (approximately 60 meters). This capability underscores the operational challenges posed by fog: visibility below 550 meters prohibits aircraft landings and takeoffs.

In addition to the airport data, daily sea surface temperature (SST) measurements from the Pula Bay oceanographic station were included. These SST values, recorded at 07:00, 14:00, and 21:00 local time from January 1, 2001, to December 31, 2020, were supplemented with reprocessed satellite SST data from the Copernicus Marine Data Store (https://data.marine.copernicus.eu/). This gap-free dataset, which has been optimally interpolated with a grid resolution of 0.05° (Merchant et al., 2019), provides a comprehensive view of sea surface temperatures. Two coastal areas were selected for analysis: one to the west of the airport, encompassing the open Adriatic Sea, and the other to the east, covering the Kvarner Gulf (Figure 1). These regions were chosen to calculate the average spatial SST for a given day and evaluate their influence on fog formation. The selected areas are representative of the nearshore waters where the prevailing winds most frequently originate.

To identify the synoptic wind and pressure fields associated with fog occurrence at Pula Airport and across the Mediterranean region, 10-meter wind and mean sea-level pressure (MSLP) data were sourced from the fifth generation of ECMWF's ERA5 reanalysis. This reanalysis provides a comprehensive record of global climate and weather from the last 4 to 7 decades. ERA5 integrates observational data with atmospheric models to deliver detailed and accurate assessments of past weather. It has a horizontal resolution of 0.25° for latitude and longitude, a temporal resolution of one hour, and a vertical resolution based on 37 pressure levels (Hersbach et al., 2020a; 2020b). The study area spans from 6°W to 42°E and 30°N to 48°N (Figure 1a, inset map), encompassing the region where key synoptic processes influencing the Adriatic Sea predominantly occur. The analysis covers a 40-year period from 1979 to 2019, providing a comprehensive temporal dataset for assessing atmospheric conditions. At the same time, this area optimizes the calculation time. To manage the large datasets of 10-meter wind and MSLP and classify them into spatio-temporal patterns that shed light on atmospheric conditions favoring fog formation at Pula Airport, the Growing Neural Gas Network (GNG) method was employed. GNG is an unsupervised artificial neural network that clusters high-dimensional input data by reducing its dimensions and grouping it into best matching units (BMUs) (Fritzke, 1995).

Unlike traditional neural networks with fixed structures, GNG dynamically expands by adding new neurons in response to input patterns. This ability to grow and adapt allows GNG to effectively cluster data and detect patterns and anomalies. The GNG algorithm has been successfully used to detect anomalies in Adriatic Sea data, combining various biological and oceanographic inputs (Šantić et al., 2021; Džoić et al., 2022).

In this study, the methodology described in Matić et al. (2022) was applied to a high-dimensional, hourly, 40-year dataset comprising wind components u and v, analyzed separately for each month of the year. Prior to implementing the GNG algorithm, the wind data was arranged in such a way that two columns represented the spatial variations of u and v, while rows corresponded to temporal instances. Wind data over land was excluded and assigned as NaN values to reduce calculation time. This exclusion did not affect the results, as the study's primary focus was on the synoptic-scale influences that generate specific wind patterns conducive to the formation of fog and mist. Over the sea, the winds are very homogeneous and are often directly related to large-scale synoptic systems such as cyclones or anticyclones, whereas over land, the influence of topography and vegetation introduces noise, masking these processes. The proximity of the airfield to the sea and the flat, low-lying terrain in the direction of prevailing winds (Figure 1b) justified this simplification of calculations. The GNG algorithm, implemented using the NeuPy Python library and parameterized following Matić et al. (2022), was used to calculate 9 BMUs per month for each month of the year. These BMUs were then linked to corresponding mean sea level pressure (MSLP) fields. The temporal sequence of BMUs was utilized to compute an average pressure field for each BMU, offering a detailed representation of atmospheric patterns associated with fog formation.

Data processing and visualization were conducted using Python and MATLAB, with MATLAB employing the M_map mapping package (Pawlowicz, 2020), available at www.eoas.ubc.ca/~rich/map.html.

3 Results and discussion

3.1 Climatological analysis

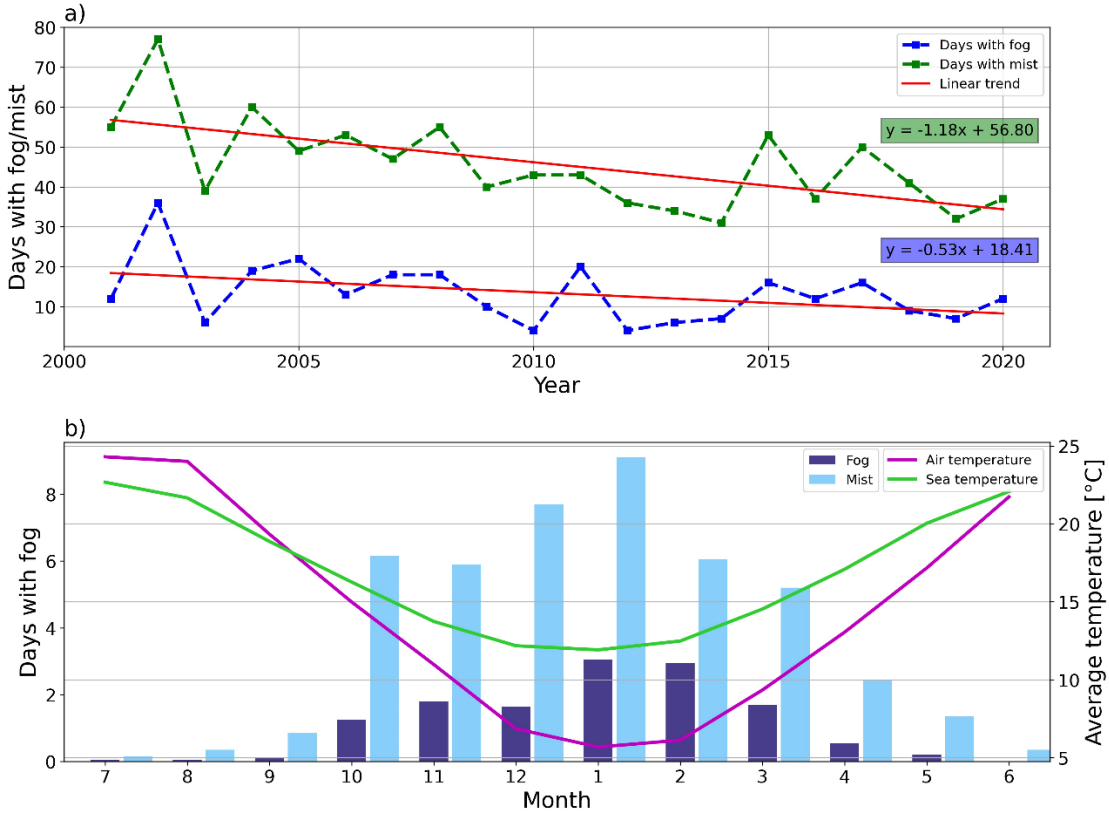

Figure 2. a) Annual number of days with fog (blue line) and mist (green line) at Pula Airport, 2001-2020. with associated linear trends and trend equations. b) Average monthly number of days with fog and mist at Pula Airport, the average sea temperature measured at the oceanographic station in Pula Bay and the average air temperature measured at the Pula Airport, 2021-2020. The graph is centered on the boreal winter.

To comprehensively analyze fog occurrence over Pula Airport, a climatological analysis was conducted at both large and small scales. Figure 2a illustrates the annual number of days with fog and mist from 2001 to 2020. A "fog day" is defined as any day with at least one METAR report indicating visibility below 1 km and the presence of fog at the airport. Similarly, a "mist day" is defined as any day with a METAR report indicating visibility between 1 km and 5 km, accompanied by mist observation, consistent with aeronautical meteorology definitions. This approach excludes cases where reduced visibility was caused by precipitation, such as rain or drizzle. On average, Pula Airport experiences 13.4 fog days and 45.6 mist days per year; however, this number is steadily decreasing, as indicated by the pronounced negative trend. The Mann-Kendall statistical significance test shows that this result is statistically significant at the 95% confidence level. A detailed evaluation of the linear trend indicates that the average number of fog days decreased by more than 10 days, from 18.4 in 2001 to 8.3 in 2020, with a slope coefficient of -0.53. Similarly, the average number of mist days declined by over 22 days, from 56.8 in 2001 to 34.4 in 2020, with a slope coefficient of -1.18. The larger absolute value of the slope coefficient for mist suggests that the average number of mist days is declining at a faster rate.

A seasonal analysis (Figure 2b) reveals that over 90% of fog and mist events occur between October and March. January accounts for the highest frequency of fog (23% of days) and mist (20% of days), followed by February (21% and 13%, respectively), with December notable for mist (17%). In March, October, and November, fog and mist occur on 12–13% of days. Fog is rare from April to May and almost absent from June to September; for example, no fog was observed in June during the analyzed period. The annual distribution of fog at Pula Airport is also comparable to the annual distribution of fog events at Zagreb Airport (Zoldoš and Jurković, 2016). A summary of the data shows that during the climatological summer (June-July-August), fog occurrence can be expected approximately every six years. Mist follows a similar seasonal pattern but is more frequent overall. In recent decades, January and February have swapped positions as the months with the highest frequency of fog. While February used to be the foggiest month at Pula Airport with an average of 3.5 foggy days (Stipaničić, 1972), climatological results have shown us that January has become the foggiest month with 3.05 foggy days. The frequency of fog persistence, which is defined as fog occurrence on two consecutive days, is shown in Figure 3. As expected based on previous findings about fog characteristics, persistence can be expected only in the colder part of the year (October-April). From May to September, there have been no recorded instances of fog occurring on two consecutive days. Stable anticyclonic conditions during the cold season are most conducive to fog persistence.

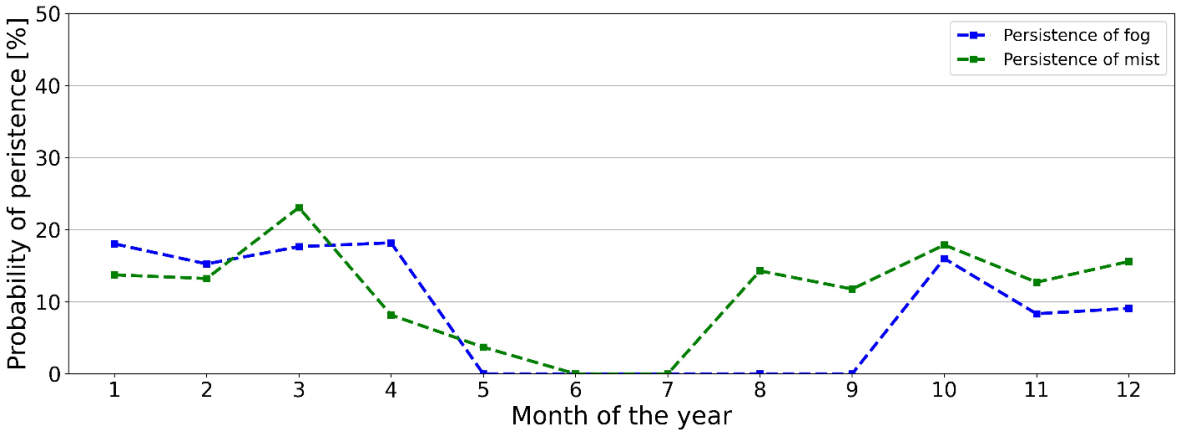

Figure 3. Yearly distribution of the climatological probability of persistence (fog occurrence on two consecutive days) of fog and mist at Pula Airport, 2001-2020. The probability of persistence is defined as the number of days with persistence relative to the total number of days with fog in a given month. Cases where a single fog event was present around midnight (and thus spanned two days) were not counted as persistence.

Wind is a critical factor influencing the formation and persistence of fog, as turbulence from wind shear significantly impacts the height of the stable boundary layer. To understand this relationship, the statistical characteristics of wind during fog episodes were analyzed. Figure 4 shows wind distributions (data from METAR reports) for all conditions and for fog/mist conditions in a wind rose plot. In general, the dominant wind at Pula Airport is the NE (*bora)*, which can easily reach speeds greater than 10 m s^{-1}. Other frequently observed winds include westerlies, resulting from the interaction of Etesian winds with the sea breeze circulation (Pandžić and Likso, 2005; Klaić et al., 2009), as well as north-northeasterly and southeasterly winds. Winds from the northwest and southwest are relatively rare. The wind rose for fog conditions (Figure 4b) contrasts sharply with general conditions; W/NW winds are the most common (accounting for 47.7% of measurements). These winds blow from the direction of the open sea, whereas easterly winds

blow from Kvarner Bay, characterized by deeper waters and numerous islands. In some cases fog also forms under light easterly winds, typically below 3 m s^{-1}, although westerly fog events are often accompanied by wind speeds exceeding this threshold. Southerly winds are rarely associated with fog at Pula Airport.

Mist conditions show a different wind pattern (Figure 4c). Unlike fog, mist frequently occurs with easterly winds, which account for 28.8% of observations. This is consistent with the higher overall occurrence of mist compared to fog (Figure 2). Further analysis of the relationship between wind and visibility/cloud base in fog conditions (Figure 5a-d) highlights the rarity of fog in situations with northerly winds. The scatter plot of visibility and wind speed confirms the existence of an optimal range of wind speeds conducive to fog, with most fog events occurring at wind speeds between 0 and 2 m s^{-1}. The same is also observed for low clouds (lower than 200 m) — the majority of low cloud bases were observed at wind speeds of 1 m s^{-1} or less, some between 1 and 2 m s^{-1}, and very few cases at higher wind speeds. The absence of cloud bases above 300 m at wind speeds higher than 2 m s^{-1} is interesting. Higher wind speeds indicate stronger advection, and personal communication from forecasters suggests that in these cases cloud bases can be very low. This is particularly evident under westerly flows, where fog is more common and where wind speeds are higher. The data for mist conditions (Figure 5e-h) leads to similar conclusions for visibility—mist occurs more frequently under westerly or easterly winds with slightly higher wind speeds than fog. Mist conditions with cloud bases above 500 m do occur but are rare, and one noteworthy difference between mist and fog is the higher number of mist events with a low cloud base during southeasterly and southwesterly winds.

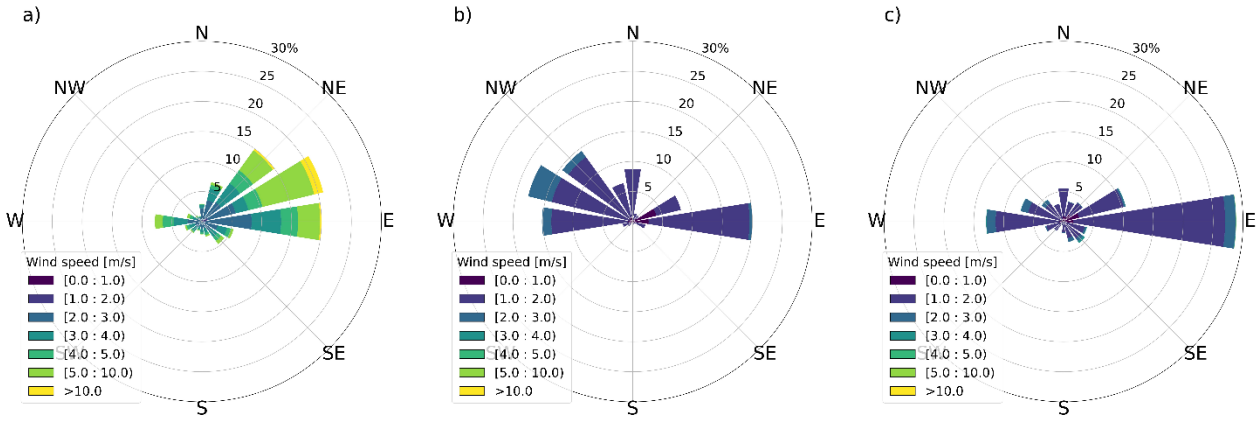

Figure 4. Wind rose plots for Pula Airport, for dataset in the period 2001-2020: (a) the whole dataset, (b) fog conditions (c) mist conditions. Data includes only reports where the variation in direction is less than 60° according to ICAO definition. These account for 74 % of total data, 36 % of data in fog conditions and 39% of data in mist conditions.

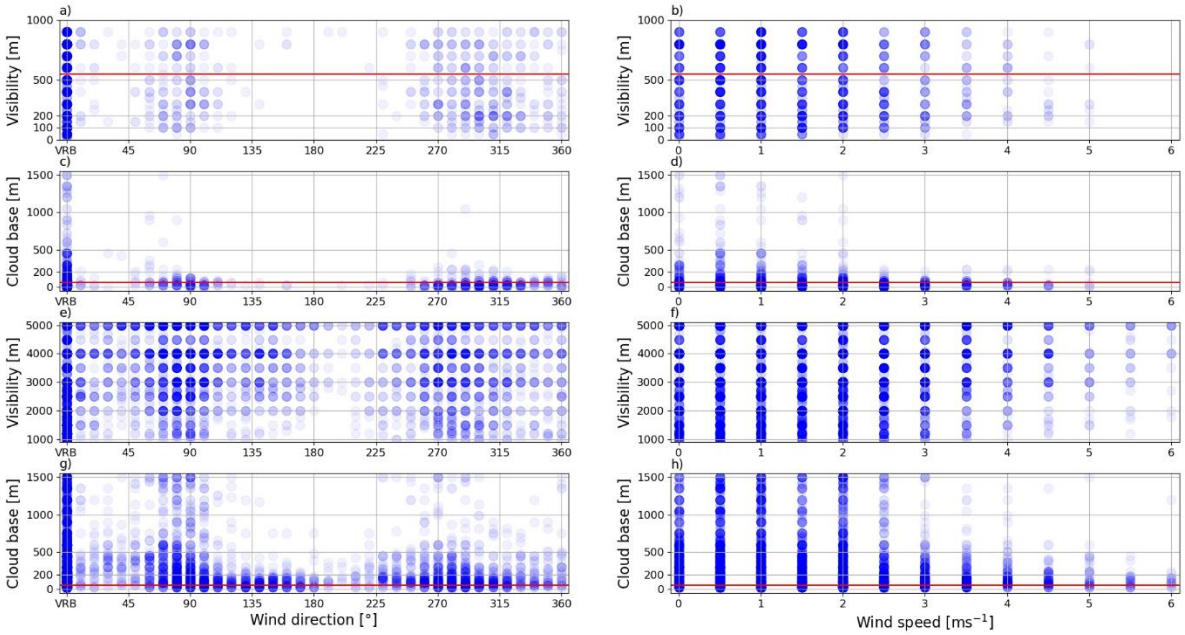

Figure 5. Scatter plots of various meteorological parameters for fog conditions (a-d) and mist conditions (e-h) at Pula Airport, 2001-2020. Circles are colored according to the frequency of data points (darker – more frequent). Red lines mark the limits for Category I takeoff-landing procedures mentioned in Chapter 2. "VRB" denotes variable wind direction (180° or more in a 2-minute interval) according to definition by ICAO (International Civil Aviation Organization).

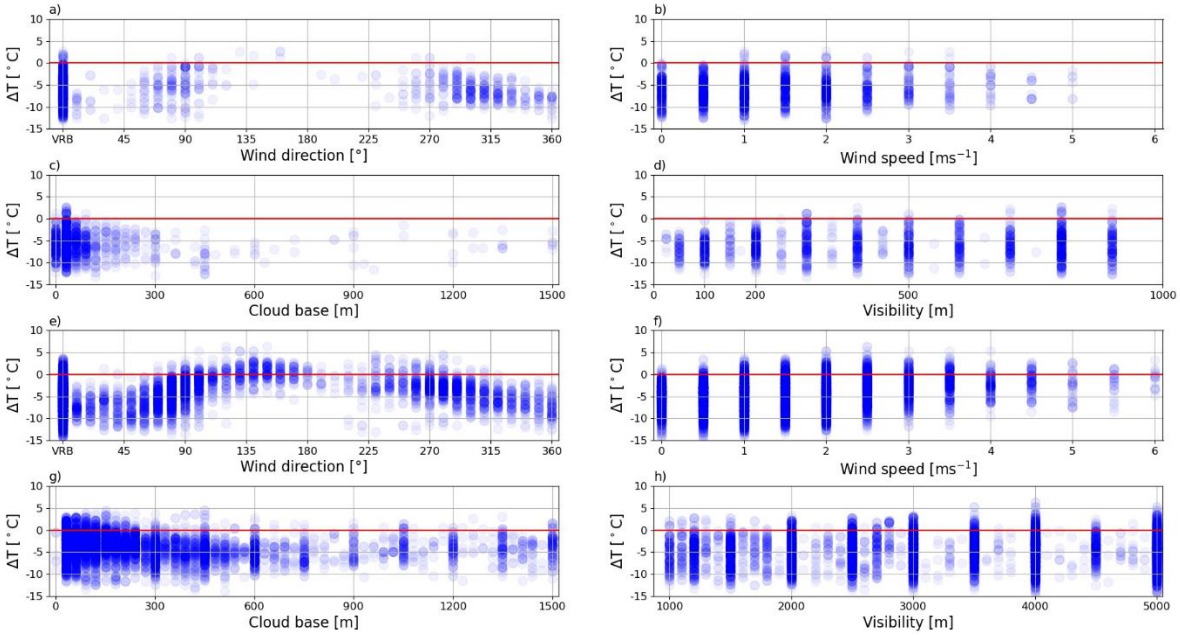

Figure 6. Scatter plots of air-sea temperature difference between Pula Airport and Pula oceanographic station and various meteorological parameters at fog initiation (a-d) and mist initiation (e-h), 2001-2020. Circles are colored according to the frequency of data points (darker – more frequent). Red lines mark the 0 °C difference between air and sea temperature. "VRB" denotes variable wind direction (180° or more in a 2-minute interval) according to definition by ICAO (International Civil Aviation Organization).

Fog occurrence can also be analyzed by examining conditions leading up to or at the time of its formation, as demonstrated in previous studies (Tardif and Rasmussen, 2007; Veljović et al., 2015; Zoldoš and Jurković, 2016), or by investigating the difference between air and sea surface temperature for marine fog (Li et al., 2022). In this study, SAT data from METAR reports at Pula Airport were compared with SST measurements from the oceanographic station in Pula Bay. Figures 6a-d depict scatterplots of SAT-SST differences and various parameters at fog initiation (first METAR report with visibility <1000 m), while Figures 6e-h present similar data for mist initiation.

The majority of fog and mist events occur under negative SAT-SST differences, indicating that the sea surface is warmer than the overlying air. Fog rarely forms during southerly winds, but mist is more common in these conditions, particularly under southeasterly winds (Figure 6e). For southeasterly, southerly, and southwesterly winds with mist, the SAT-SST difference tends to approach 0. Among fog events, 97.4% occured with negative SAT-SST differences, with only 2.6% forming under conditions where SAT is equal to or warmer than SST. In mist cases, the proportion of positive or zero SAT-SST differences is slightly higher (7.4%) but still strongly favors conditions with warm sea and cooler air. At Pula Airport, fog is more common at wind speeds above 3 m s^{-1} than in continental areas such as Zagreb Airport (Zoldoš and Jurković, 2016), but less common than in coastal regions such as California, where fog occurs at speeds above 10 m s^{-1} (Filonczuk et al., 1995). Fog rarely occurs in calm conditions, suggesting an optimal wind speed range for its formation and warranting further exploration, as the role of wind speed on turbulence and surface heat fluxes, as highlighted by Gultepe et al. (2007), significantly influences fog. While the influence of SST was initially assessed by comparing SAT measurements from the airport with SST data from the oceanographic station, a more comprehensive understanding is obtained by examining the effect of the sea to the west and east of the airport. To achieve this, satellite-derived SST values for the regions west and east of the airport (Figure 1b) were analyzed. These areas correspond to the directions of the two prevailing winds most commonly associated with fog formation at Pula Airport. Scatterplots of SAT versus SST were generated for the eastern and western regions, encompassing all observations, as well as those specifically under fog and mist conditions (Figure 7). A visual analysis indicates that fog and mist typically form when SAT-SST pairs are associated with lower values. A more detailed analysis reveals that fog data points (red dots) in the western region are more dispersed, indicating greater variability in SST for the same SAT, while the eastern region shows a more consistent SST-SAT relationship. Statistical analysis supports this observation, with the standard deviation of SST for fog observations being 3.55 °C in the western area and 3.37 °C in the eastern area. For mist, the standard deviation is 4.03 °C in the western area and 3.83 °C in the eastern area. To further investigate the role of SST in fog formation in fog formation, differences in SST between the western and eastern regions were analyzed under various conditions (Figure 8). When neither fog nor mist is present, SST in the western area is slightly higher than in the eastern area. During fog events, however, the pattern reverses, with SST being higher in the eastern area. In contrast, mist typically occurs when SST is higher in the western area than in the eastern area. These differences align with the prevailing wind directions observed during fog and mist events (Figure 4). During fog, winds that are predominantly from the west to northwest (W-NW) promote cooling in the western area. Winds from the east (E) during mist contribute to reduced SST in the eastern region. Despite these variations, the SST differences between the two areas are small, rarely exceeding 0.5 °C.

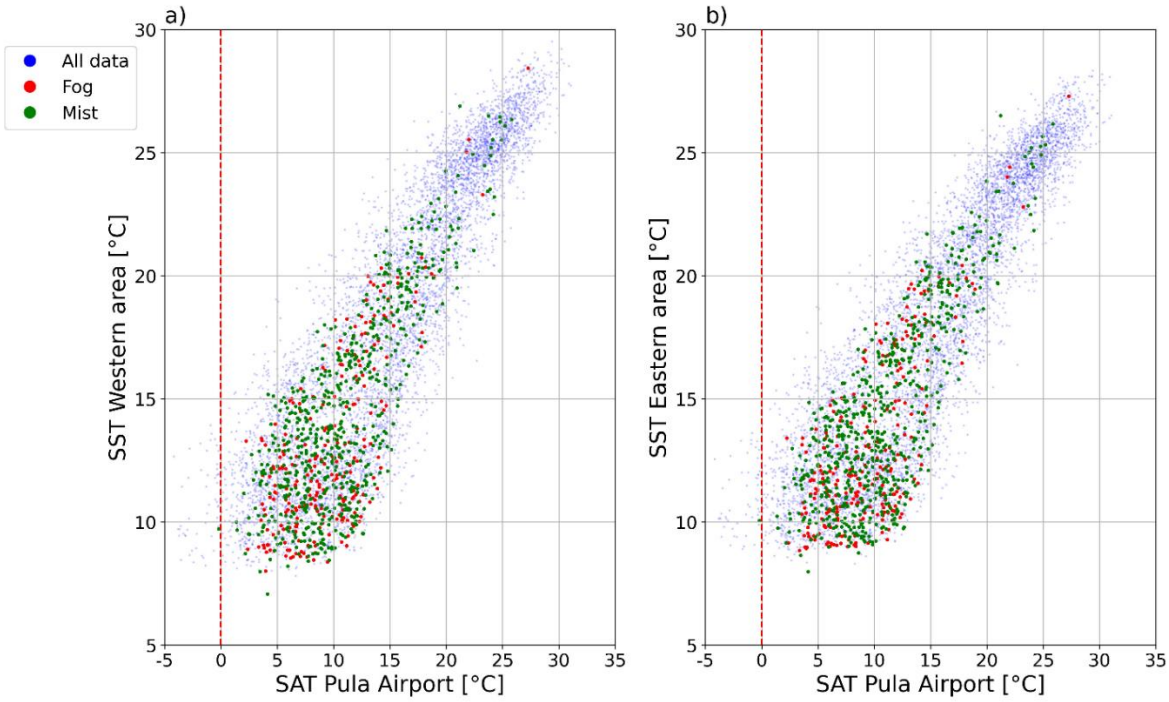

Figure 7. Scatter plots of satellite sea surface temperature (SST) for western area (a) and eastern area (b), and surface air temperature (SAT) at Pula Airport, 2001.-2020.

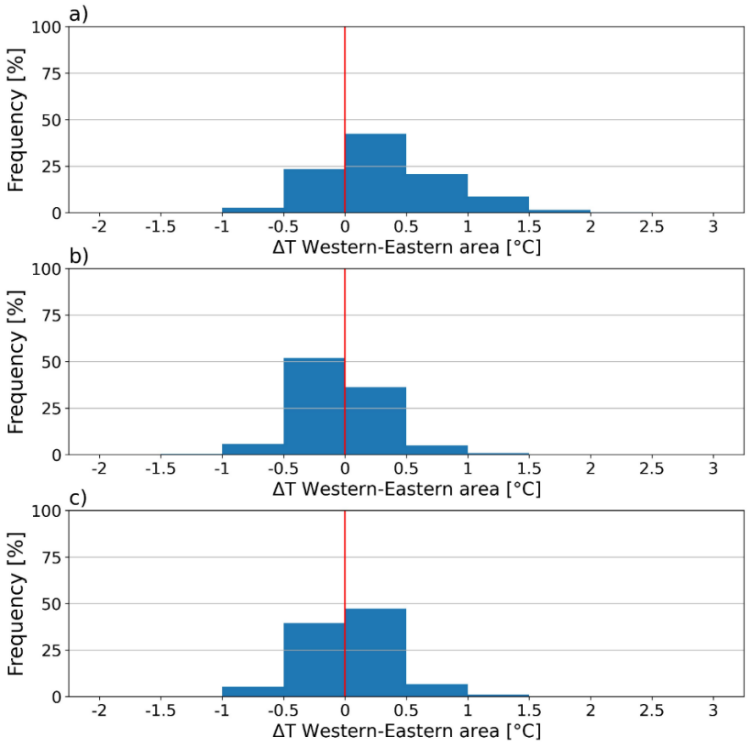

Figure 8. Histograms of satellite SST difference between the western and eastern area for observations without fog or mist (a), fog (b) and mist(c).

3.2 GNG analysis of synoptic weather patterns

In this analysis, the GNG method was applied to identify characteristic temporal and spatial patterns in wind and MSLP fields associated with the formation of fog and mist in the Pula region. The analysis was conducted on a monthly basis, processing data for each month (e.g., all January data, all February data) separately. This approach was chosen to improve the interpretability of the results, to take seasonality into account and to reduce the computational effort, especially given the large size of the hourly dataset. To save resources, the GNG algorithm was applied exclusively to 10 m wind data from ERA5, with the derived pressure fields being extrapolated afterwards. The derived pressure field corresponds to the mean pressure field associated with each BMU. Once the BMUs were identified, all pressure fields corresponding to the time instances of each BMU were retrieved and averaged to calculate the mean pressure field for each BMU. To obtain an appropriate synoptic situation with large wind systems, such as anticyclones and cyclones affecting the northern Adriatic, a large area in the Mediterranean was selected for analysis (Figure 1b). The analysis utilized 40 years of ERA5 data (1979–2019), providing extensive time series data to enable the GNG algorithm to derive robust and accurate spatio-temporal patterns. Notably, there is a one-year discrepancy between the ERA5 dataset and the fog dataset (2020) due to the GNG analysis being completed before this study began, and the computational resources required for a new analysis were unavailable. Since the wind was the primary variable and the MSLP was derived by averaging numerous synoptic situations, the wind had the dominant influence. This approach excluded the occurrence of extreme cyclonic systems (MSLP < 1000 hPa) or anticyclonic (MSLP > 1030 hPa) from the results. For example, deep cyclones, which are extremes, are smoothed, and while BMUs can indicate their locations, the exact pressure values are not retained. However, from a conceptual point of view, the interaction between high and low pressure systems and the location of these systems and their associated winds match well with the climatology of the region.

This process generated 9 Best Matching Units (BMUs) for each month (a total of 108 BMUs) distributed across hourly data, representing the weather patterns with the highest variance. Hourly data were then aggregated into daily data by identifying the most frequently occuring BMU within a day. For the 2001–2019 period, each day with fog or mist was assigned to its corresponding dominant BMU, providing a synoptic weather pattern classification for fog and mist days at Pula Airport. To focus on the prevailing synoptic patterns that contribute to the formation of fog and mist, the months from October to March (Figure 2b) were examined in more detail (Table 1). In this way, 85 % of the variability could be captured. Then, for each month, the first BMUs whose sum of their contributions to the variability exceeded the threshold of 60 % were selected. In this way, a total of 18 BMUs were included in the further analysis, which is significantly fewer than 54 BMUs (6 months multiplied by 9 BMUs). By selecting 2 to 4 BMUs for each month based on the criteria described above, the study captured more than 60 percent of the events for each analyzed month.

Table 1. Display of the most frequent Best Matching Units (BMUs) (the first BMUs for each month whose sum of their contributions to the variability exceeded the threshold of 60 %) describing the prevailing synoptic weather pattern during the days with fog and mist for the selected month at Pula Airport, 2001-2019. The slope coefficients describe the linear trends of the most common BMUs, i.e. the yearly change in frequency, and they are also used to generate the graphs of the linear trends in Figure 14.

Month	BMU	Synoptic pattern	Wind	Slope coeff.	Frequency (fog)		Frequency (mist)	
					#	%	#	%
January	BMU-1-6	Quasi-non-gradient-field	WNW, W	-0.390	30	54 %	68	39 %
	BMU-1-8	Cyclone over northern Adriatic (MSLP<1008 hPa)	NW	0.107	11	20 %	39	23 %
February	BMU-2-5	Anticyclone over central/western Europe (MSLP>1028 hPa)	NE, NNE	0.006	8	16 %	13	12 %
	BMU-2-6	Quasi-non-gradient-field	SSW	-0.138	17	33 %	36	32 %
	BMU-2-7	Cyclone over northern Adriatic (MSLP<1008 hPa)	NW	-0.025	7	14 %	59	38 %
March	BMU-3-1	Anticyclone over southeastern Europe (MSLP>1022 hPa)	SSE	-0.572	16	16 %	5	16 %
	BMU-3-3	Cyclone over northern Adriatic (MSLP<1006 hPa)	SE	-0.051	6	19 %	25	25 %
	BMU-3-8	Quasi-non-gradient-field	SSE	0.255	11	35 %	31	39 %
October	BMU-10-1	Anticyclone over southeastern Europe (MSLP>1018 hPa)	NE	0.158	4	16 %	13	11 %
	BMU-10-5	Anticyclone over southeastern Europe (MSLP>1020 hPa)	SE	-0.272	10	40 %	38	32 %
	BMU-10-6	Quasi-non-gradient-field	SE	-0.051	4	16 %	27	23 %
November	BMU-11-5	Anticyclone over eastern Europe (MSLP>1024 hPa)	SE	0.251	8	24 %	23	21 %
	BMU-11-7	Quasi-non-gradient-field (MSLP>1022 hPa)	WSW	-0.415	6	18 %	29	26 %
	BMU-11-9	Anticyclone over southeastern Europe (MSLP>1026hPa)	ENE	-0.041	11	33 %	28	25 %
December	BMU-12-1	Anticyclone over southeastern Europe (MSLP>1026 hPa)	S	-0.000	7	21 %	31	21 %
	BMU-12-3	Cyclone over southern Adriatic (MSLP<1008 hPa)	NE	0.266	5	15 %	23	15 %
	BMU-12-4	Cyclone over the Tyrhennian Sea (MSLP<1008 hPa)	NE	-0.470	6	18 %	14	9 %
	BMU-12-8	Anticyclone over central and eastern Europe (MSLP >1030 hPa)	NE	-0.130	3	9 %	23	15 %

The analysis of synoptic patterns associated with fog formation (Table 1) indicates that in January, the dominant conditions favoring fog and mist in Pula are characterized by a quasi-non-gradient field across the region (BMU-1-6, Figure 9a), with a very weak mean pressure gradient (Belušić Vozila et al., 2021). This stable atmospheric pattern supports the persistence of calm and stagnant air masses over Pula, limiting the dispersion of moisture and pollutants and thereby enabling fog formation. The second most common synoptic pattern conducive to the formation of fog and mist features a cyclone over the northern Adriatic (BMU-1-8, Figure 9c). Both synoptic patterns support weak WNW/NW winds over the Istrian peninsula (Figure 9b and 9d). A similar synoptic pattern persists during the transition

into February and March. The cyclone over the northern Adriatic is the most frequent pattern suitable for the formation of mist in February (BMU-2-7, Figure 10a) and the second most frequent in March (BMU-3-3, Figure 10e). The difference is the prevailing NW wind in February (Figure 10b), while March is characterized by SE winds (Figure 10f). The quasi-non-gradient pressure field is the most common pattern favorable for both fog and mist formation in March (BMU-3-8, Figure 10g), and the second most common for fog and the most common for mist in February (BMU-2-6, Figure 9g). SSW winds are observed in February (Figure 9h), whereas March is associated with weaker SSE winds (Figure 10d). In addition to the quasi-non-gradient field, favorable synoptic patterns in both February and March also include anticyclones over continental Europe (BMU-2-5, Figure 9e and BMU-3-1, Figure 10c).

Fog events are rare in Pula from April to September, and as a result, the BMU analysis does not reveal clear patterns. The infrequent occurrence of fog during this period is attributed to lower relative humidity and the more stable atmospheric conditions typical of summer in the region. However, local factors, such as the sea/land breeze, may influence fog formation. Therefore, any analysis based on data from these months should be interpreted with caution, as the number of recorded fog events is limited.

At the beginning of October, synoptic conditions favorable for the occurrence of fog and mist in Pula are typically characterized by high pressure over continental Europe, with the most common pattern being the center of the high-pressure system positioned over southeastern Europe, which supports SE winds (BMU-10-5, Figure 11c and 11d). This anticyclonic pattern persists into November, accompanied by a strengthened pressure field and intensified pressure gradients over the central Mediterranean, conditions which promote fog development in the region (BMU-11-9, Figure 12e and 12f). The intensified synoptic pressure gradients over the central Mediterranean contribute to increased NE wind patterns. This increased wind activity can result in moist air being transported from the sea to the coastal regions, providing an additional source of moisture for fog formation. The convergence of air masses along these enhanced pressure gradients likely induces upward motion of air, which can result in adiabatic cooling and an increase in relative humidity, creating conditions favorable to fog and mist formation. Pula's coastal location amplifies the influence of the anticyclone. Coastal areas are more prone to temperature inversions due to the sea's heat retention, which reduces temperature fluctuations. Anticyclonic conditions over Eastern Europe combined with coastal geography create an environment where cool, moist air is trapped near the surface, favoring the formation of fog. The conditions that favor mist formation are varied; the most common synoptic pattern is the one where the high-pressure area is located over the western Mediterranean and WSW winds over the Istrian peninsula. In addition to the anticyclone, a quasi-non-gradient field is also present in October and November (BMU-10-6, Figure 11e, 11f and BMU-11-7, Figure 12c and 12d). In December, the prevailing synoptic weather patterns associated with fog and mist become harder to identify, with BMUs more evenly distributed and more dynamic conditions, similar to those in February and March. Nonetheless, the most frequent synoptic pattern for fog and mist (BMU-12-1, Figure 13a and BMU-12-8, Figure 13g) has anticyclonic characteristics. Under these conditions, the Pula region is under the influence of a pressure ridge, with the prevailing weak wind patterns from the S and NE further increasing the probability of fog formation (Figure 13b and 13h). Compared to earlier months, cyclones also play a more pronounced role in

December's fog and mist formation. This influence is observed in two ways: weak NE winds associated with cyclonic conditions in the southern Adriatic (BMU-12-3, Figure 13c, 13d) and stronger NE winds due to cyclonic conditions in the Tyrrhenian Sea (BMU-12-4, Figure 13g, 13h).

In summary, most fog and mist events during the cold season occur under stable anticyclonic or quasi-non-gradient conditions (13 total), though some events also occur under low-pressure conditions (5 total). WNW/W winds are most common in January and February under quasi-non-gradient fields and they contribute significantly to fog formation. SE winds dominate in March and October under anticyclonic conditions. Northeasterly winds are predominant in December, often in conjunction with anticyclones. The quasi-non-gradient field is the most-frequent weather situation, accounting for 40% of fog cases and 37% of mist cases, followed by anticyclones, which account for 39% of fog cases and 33% of mist cases. Cyclones are less common, accounting for 21% of fog cases and 30% of mist cases.

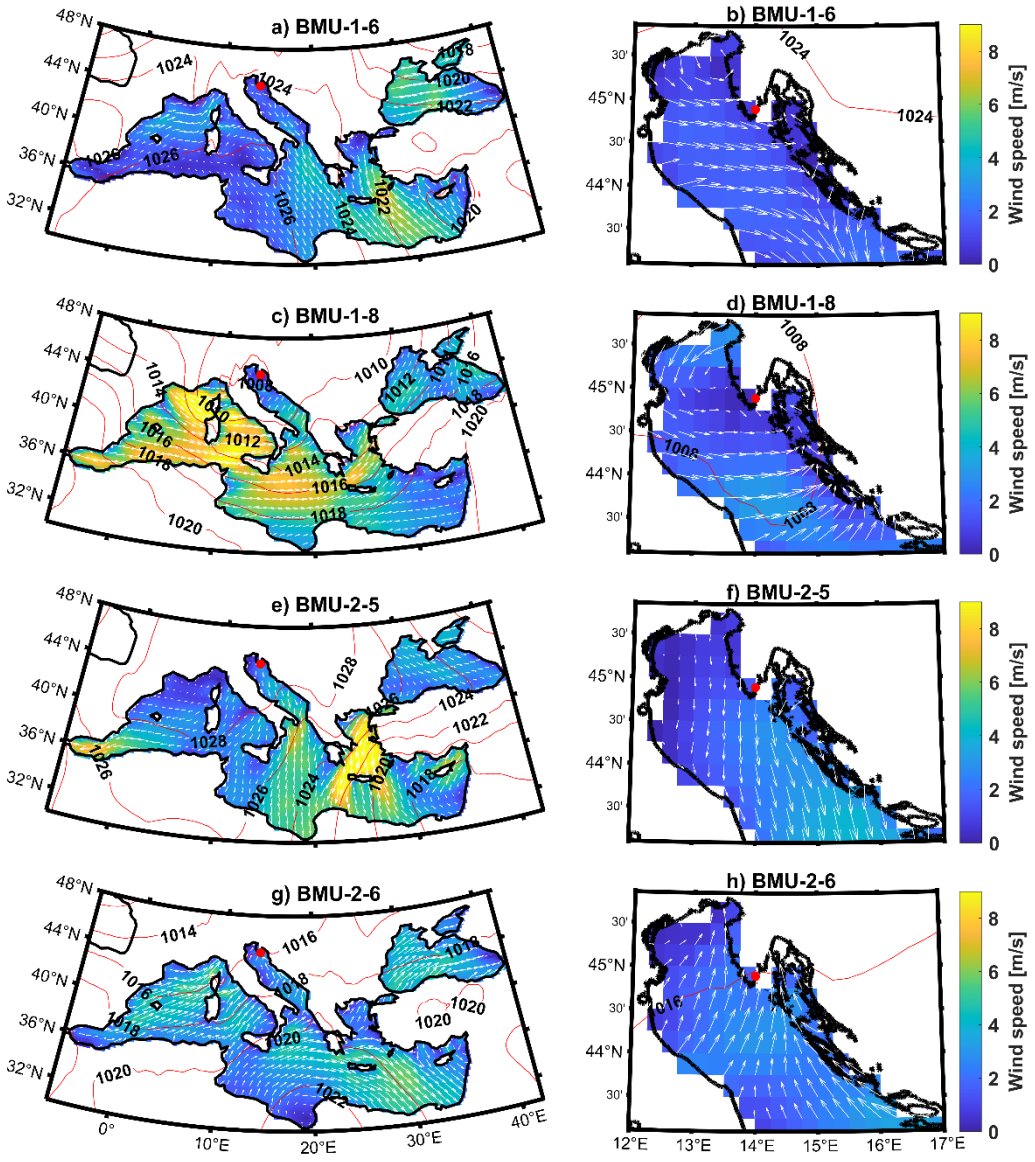

Figure 9. Prevailing Best Matching Units (BMUs) describing the synoptic patterns favoring the formation of fog and mist at Pula Airport in January (a, c) and February (e, g) for the wider Mediterranean region. The red dot marks the location of Pula Airport. The red contour lines show the mean sea level pressure (MSLP). The contours represent the amplitude of the wind speed, above which the wind vectors are represented by arrows (every third vector has been drawn). The same principle applies to the zoomed area of the northern and central Adriatic for January (b, d) and February (f, h), but here each vector is plotted.

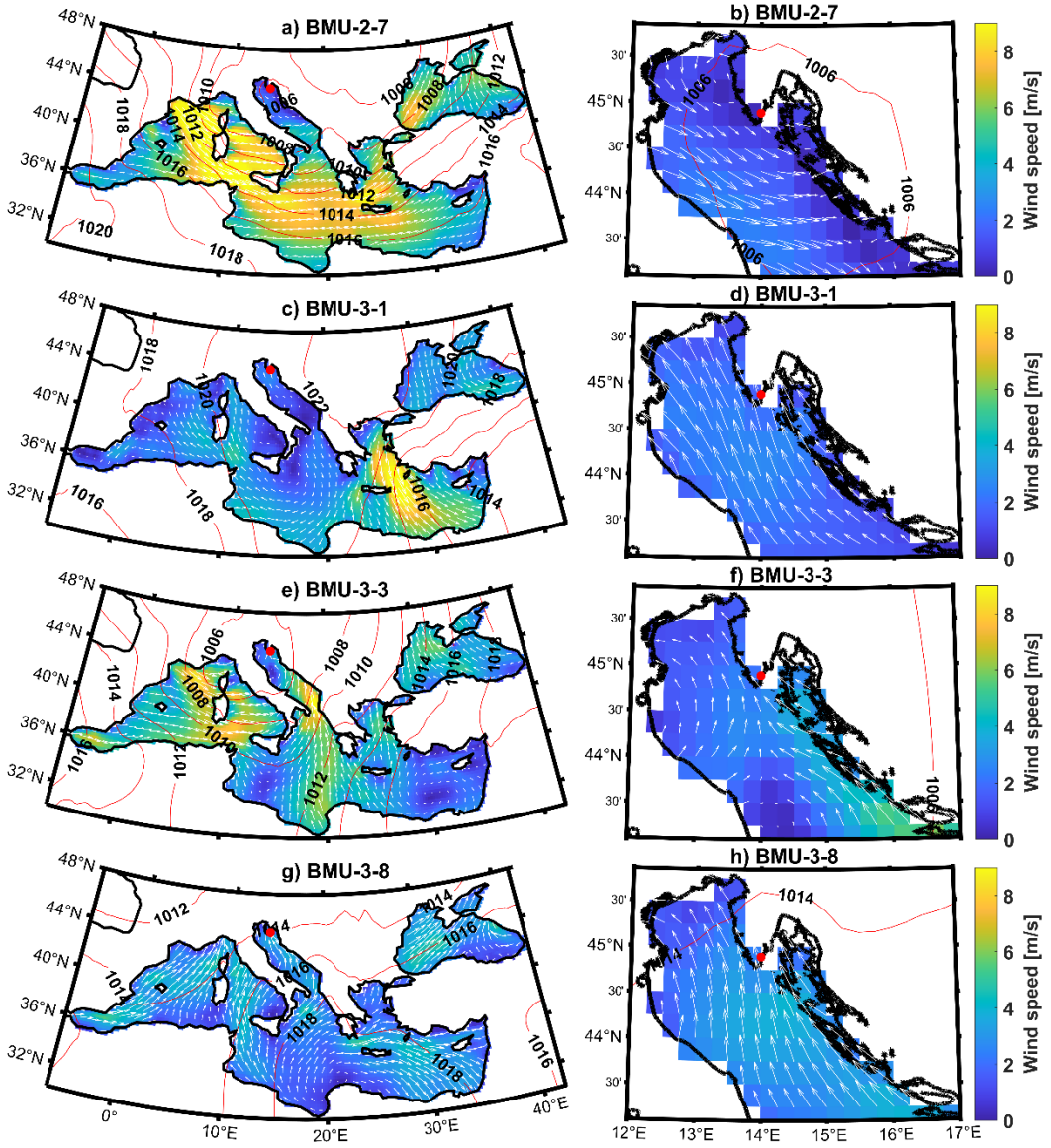

Figure 10. Similar to Figure 9, but for February (a) and March (c, e, g) in the wider Mediterranean area, and for the northern and central Adriatic: February (b) and March (d, f, h) in the zoomed-in area.

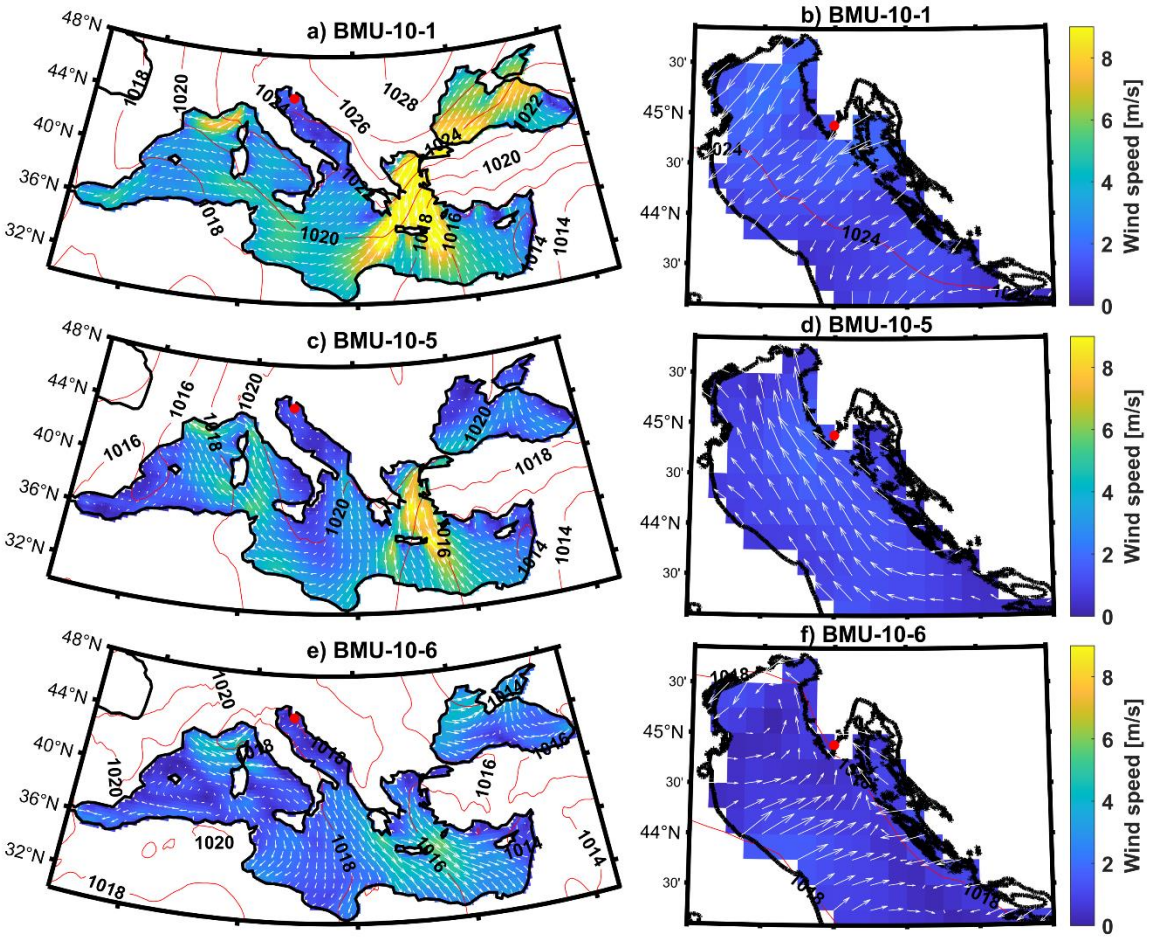

Figure 11. Similar to Figure 9, but for October: (a, c, e) show the wider Mediterranean area, while (b, d, f) focus on the northern and central Adriatic.

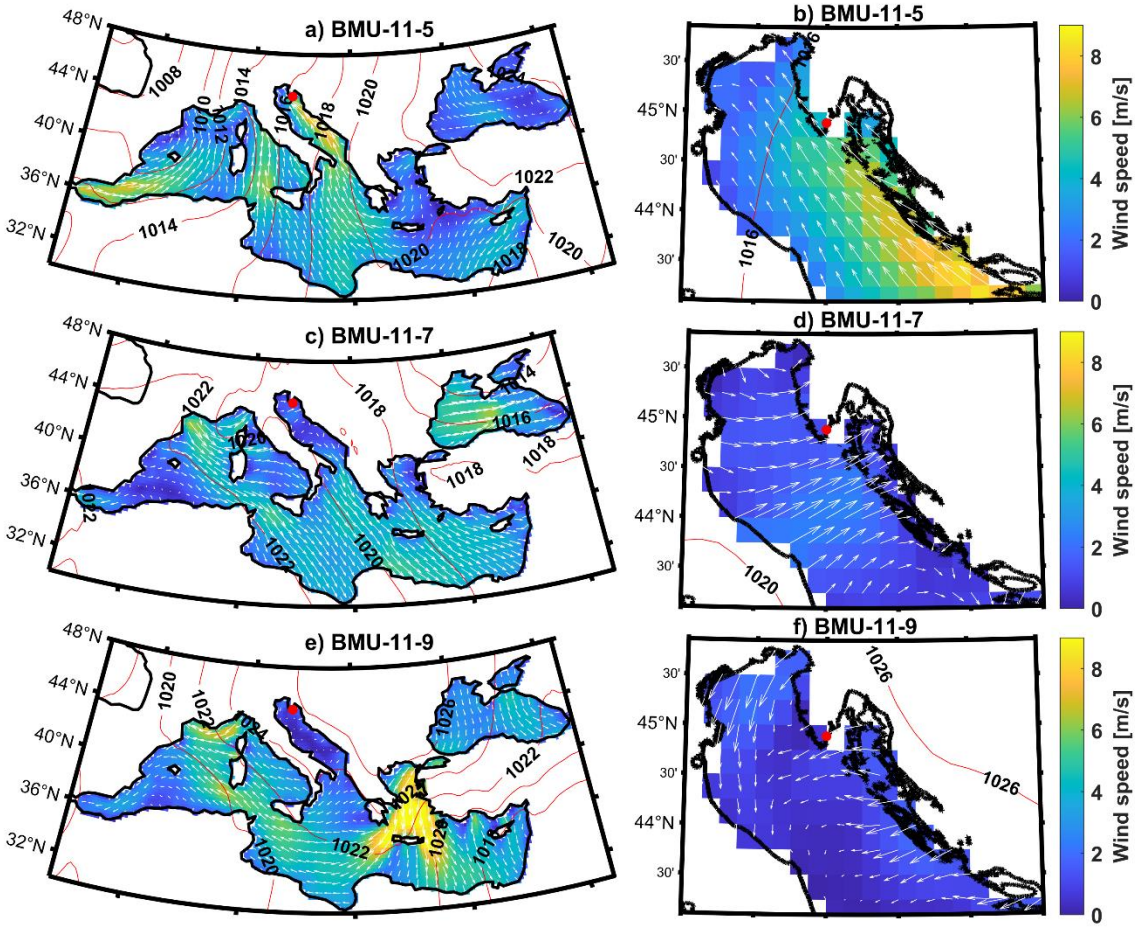

Figure 12. Similar to Figure 9, but for November: (a, c, e) show the wider Mediterranean area, while (b, d, f) focus on the northern and central Adriatic.

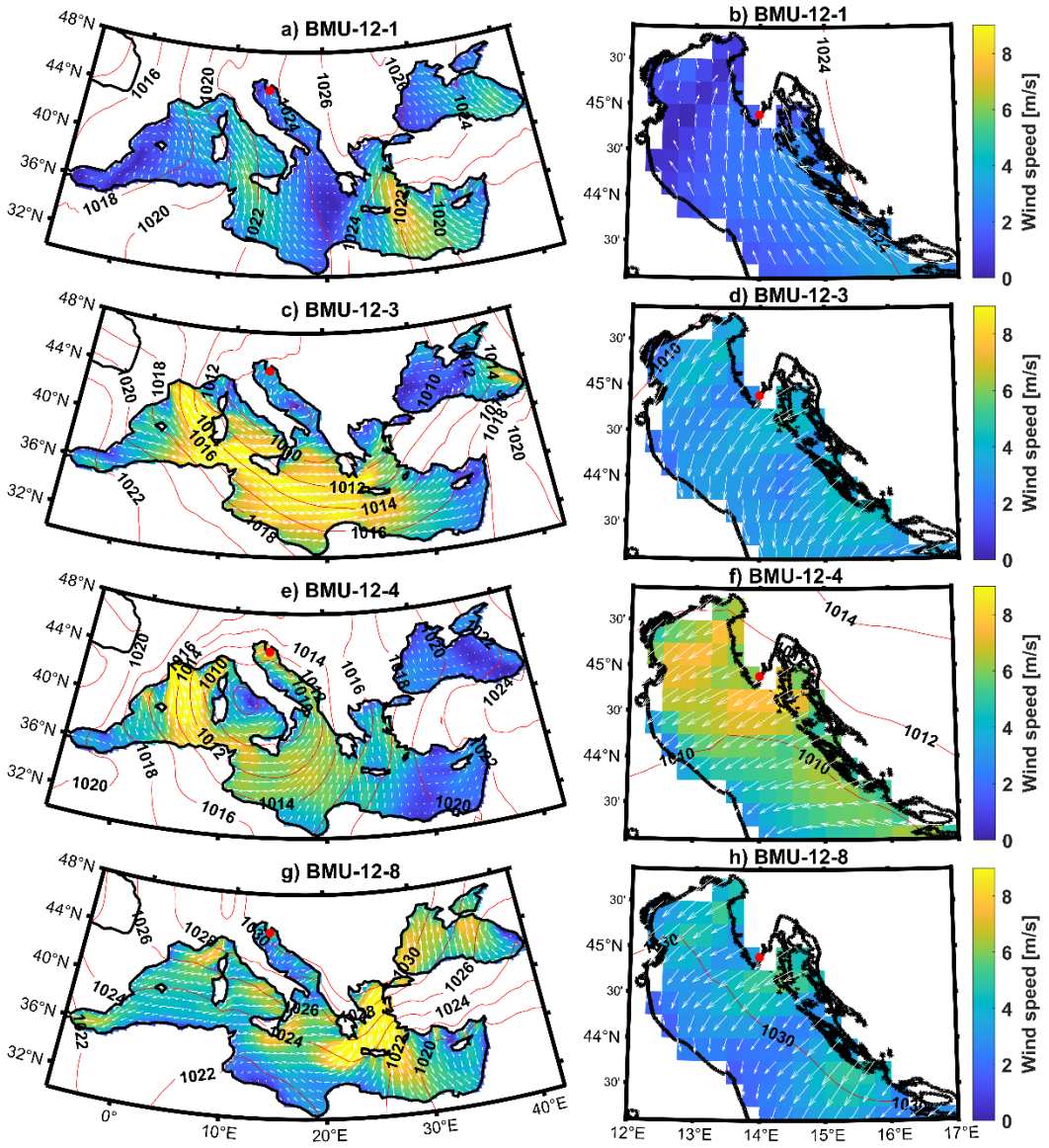

Figure 13. Similar to Figure 9 but for December: (a, c, e, g) show the wider Mediterranean, while (b, d, f, g) focus on the northern and central Adriatic.

In addition to examining the prevailing synoptic patterns during the occurrence of fog and mist, the GNG analysis also allows for the investigation of the time series of frequencies of individual BMUs. This was accomplished by first calculating the relative monthly frequency of each BMU for each year, followed by using linear regression to estimate trends and calculate slope coefficients. This process provides insights into changes in the frequency of each BMU over two decades (Table 1, Figure 14). In January, the more frequent BMU-1-6 (Figure 14a) has a strong negative trend of -0.390, while the less frequent BMU-1-8 (Figure 14b) has a weaker positive trend of 0.107. In February, the most frequent BMU-2-7 (Figure 14e) has a weak negative trend of -0.025. In March, the most frequent BMU, BMU-3-8 (Figure 14h) has a positive trend of 0.255, while BMU-3-1 (Figure 14f) has a strong negative trend of -0.572. In October, the most frequent BMU for fog and mist (BMU-10-5, Figure 14j) has a negative trend (-0.272), while in November and December there is almost no trend for the most frequent BMUs (BMU-11-9, Figure 14n and BMU-12-1, Figure 14o). It can be summarized from the table that the BMUs most associated with the occurrence of fog and mist exhibit negative trends in the months with the highest share, January and February. Analyzing the data by counting positive and negative changes and grouping the synoptic patterns into three categories (cyclonic/anticyclonic/quasi-non-gradient field) reveals that out of the 18 BMUs, 8 are anticyclonic, 5 are quasi-non-gradient, and 5 are cyclonic. There is no trend for BMU-12-1 in the anticyclonic group; 3 BMUs increase in frequency and 4 BMUs decrease in frequency. In the quasi-non-gradient group, there is 1 increase and 4 decreases. Of the 5 cyclonic BMUs, 2 increase in frequency and 3 decrease. Additionally, a significant decrease (slope coefficient >0.3 or <-0.3) is observed in BMU-3-1 (anticyclonic), BMU-1-6 (quasi-non-gradient field), and BMU-12-4 (cyclonic). Positive trends do not show such large slope coefficients.

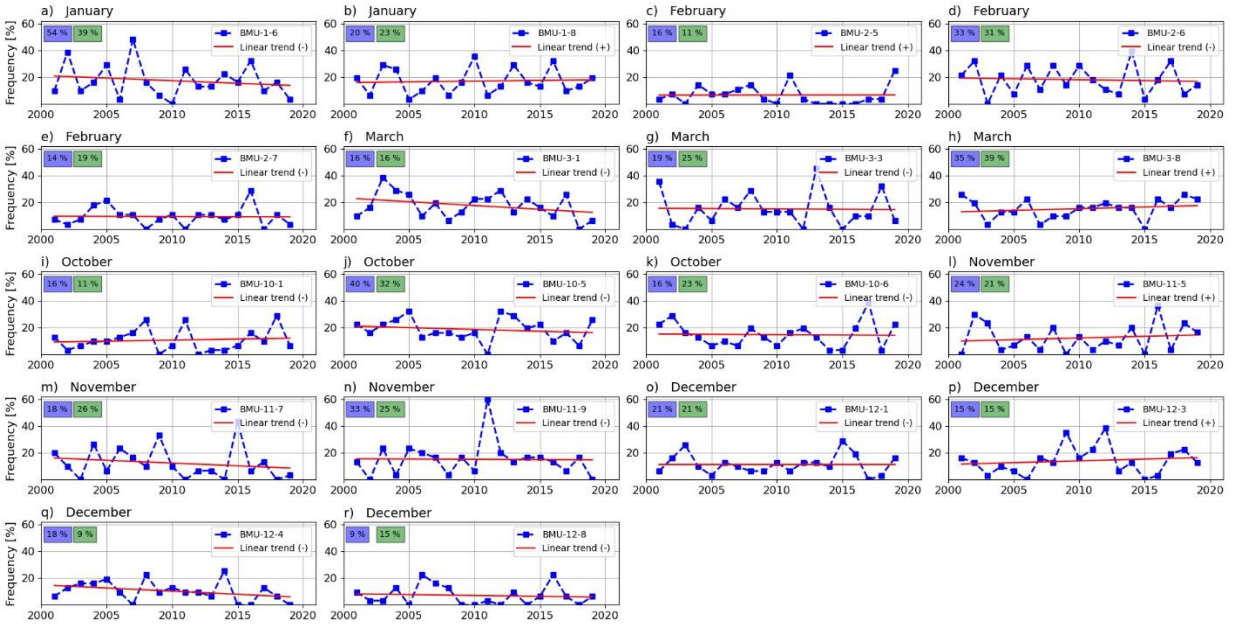

Figure 14. Relative frequencies and trends of most common (monthly share in days with fog/mist greater than 15%) BMUs for fog and mist in Pula Airport, data period: 2001-2019. Numbers shaded in blue denote the share of a BMU for fog days, numbers shaded in green denote the share of a BMU for mist days. The slope coefficient values for the linear trends can be found in Table 1.

4 Conclusion

This comprehensive climatological analysis of fog and mist occurrences at Pula Airport from 2001 to 2020 has provided valuable insights into the changing patterns of these meteorological phenomena. By combining classical statistics and neural networks, the study produced noteworthy results.

The observed statistically significant decreasing trend in the frequency of fog and mist at the airport is consistent with similar findings in Europe, such as at Zagreb Airport (Zoldoš and Jurković, 2016) and Milano Airport (Mariani, 2009). While the decrease in Zagreb and Milan is largely attributed to reduced air pollution, this conclusion is more challenging to apply to Pula. As a smaller city with less industrial development, Pula's impact on neighboring suburban and rural areas is not as pronounced. While a decrease in fog and mist frequency has been observed across Europe, the effect is more prominent in continental Europe than in the Mediterranean region (Vautard et al., 2009).

Global warming and climate change are key drivers behind the long-term decline in fog frequency. Contributing factors include rising temperatures in Pula and the surrounding Istria region (Bonacci, 2010; Šimunić et al., 2021), increased sea surface temperatures (SST) throughout the Mediterranean (Pastor et al., 2018) and global trends in ocean stratification (Li et al., 2020). Climate model reanalysis for the Adriatic Sea from 1987 to 2017 shows clearly positive SST trends, especially in summer (Tojčić et al., 2023). Positive wind trends have been observed over the sea and along the Adriatic Coast, between 0.1 and 0.2 m s-1 per decade (Tojčić et al., 2023), which could influence fog formation. Warmer SSTs reduce the temperature gradient required for fog formation and increase evaporation rates, promoting fog advection when winds are favorable. In Pula, these favorable winds, which blow over the sea, play a significant role in fog and mist formation.

Analyzing the classified synoptic patterns—a key focus of this study—reveals that the patterns conducive to fog and mist generally have a negative trend. For example, quasi-non-gradient synoptic situations, the most common favorable pattern, have shown predominantly negative trends. This decline in quasi-non-gradient synoptic situations has already been documented during the summer months (Belušić Vozila et al., 2021). As these favorable synoptic patterns decrease, the accompanying winds that facilitate the advection of evaporated moisture from the sea to the land—strongly influenced by SST and air temperatures—are also reduced. Consequently, the number of days with fog and mist is expected to decline over time.

Overall, these findings provide a strong foundation for further research, facilitating a deeper understanding of the meteorological and oceanographic factors that influence fog and mist at Pula Airport. This is especially significant as it marks the first scientific study on fog in the Pula region in over 50 years, a period during which climate change has notably impacted the local climate. Future projections suggest these changes will intensify, including lower wind speeds in coastal areas and more extreme contrasts such as increased droughts and heavy precipitation events (Tojčić et al., 2024). This study has taken on the broad task of identifying synoptic patterns conducive to fog and mist formation. Since fog and mist are mainly influenced by wind speed and moisture advection, there is potential for

coupled atmospheric-oceanographic modeling that incorporates local topography and enhances the parameterization of processes at finer temporal and spatial scales. Such advancements would provide a more comprehensive understanding of local meteorological phenomena and their implications for various applications, including aviation meteorology and environmental monitoring.

Code/data availability

All data and codes used in the analysis are available from the corresponding author on request.

Author contribution

Marko Zoldoš and Tomislav Džoić equally contributed to the conception and design of the study, material collection, data preparation, statistical and neural network analysis, creation of the figures and writing. Frano Matić contributed to the neural network analysis. All authors have read and approved the final manuscript.

Competing interests

The authors declare that they have no conflict of interest.

Acknowledgments

Frano Matić was supported in part by the European University of the Seas (SEA-EU) alliance through collaborative efforts and resources. Measurements and observations for Pula Airport were provided by the Croatian Air Navigation Service (Crocontrol Ltd.). SST data for Pula were provided by the Meteorological and Hydrological Service of Croatia (DHMZ). SST data in the Mediterranean region were downloaded from the Copernicus Marine Data Store (https://data.marine.copernicus.eu/). 10-m wind and mean sea-level pressure (MSLP) data were adopted from the fifth generation of ECMWF's ERA5 reanalysis of global climate and weather. Final proofreading (grammar/spelling check) was performed by ChatGPT from OpenAI.

References

Allan, S.S., Gaddy, S.G., Evans, J.E.: Delay causality and reduction at the New York City airports using terminal weather information systems, Massachusetts Institute of Technology, Lincoln Laboratory, Project Rep. ATC-291, 2001

Belo-Pereira, M., Santos, J.A.: A persistent wintertime fog episode at Lisbon airport (Portugal): performance of ECMWF and AROME models, Meteorol. Appl. 23, 353-370, doi:10.1002/met.1560, 2016

Bendix, J.: Fog climatology of the Po Valley, Riv. Meteorol. Aeronau. 54(3-4), 25-36, 1994

552 Belušić, A., Prtenjak, M.T., Güttler, I., Ban, N., Leutwyler, D., Schär, C.: Near-surface wind variability over the
553 broader Adriatic region: insights from an ensemble of regional climate models, Clim. Dyn. 50, 4455–4480,
554 doi:10.1007/s00382-017-3885-5, 2018
555 Belušić Vozila, A., Telišman Prtenjak, M., Güttler, I.: A weather-type classification and its application to near-surface
556 wind climate change projections over the Adriatic region, Atmosphere 12, 948, doi:/10.3390/atmos12080948, 2021
557 Bergot, T., Koračin, D.: Observation, simulation and predictability of fog: review and perspectives, Atmosphere 12(2),
558 235, doi:10.3390/atmos12020235, 2021
559 Bonacci, O. (2010): Analysis of mean annual temperature series in Croatia, Građevinar, 62(9), 781-791,
560 https://hrcak.srce.hr/59611, 2010
561 Bonacci, O.: Relationship between sea surface temperature (SST) and surface air temperature (SAT) along the eastern
562 Adriatic coast of Croatia, Vodoprivreda, 55, 325/326; 167-183, 2023
563 Duynkerke, P.G.: Radiation fog: A comparison of model simulation with detailed observations, Mon. Weather Rev.
564 119(2), 324-341, doi:10.1175/1520-0493(1991)119<0324:RFACOM>2.0.CO;2, 1991
565 Džoić, T., Zorica, B., Matić, F., Šestanović, M., Čikeš Keč, V.: Cataloguing environmental influences on the
566 spatiotemporal variability of Adriatic anchovy early life stages in the eastern Adriatic Sea using an artificial neural
567 network, Front. Mar. Sci. 9, 997937, doi:10.3389/fmars.2022.997937, 2022
568 Filonczuk, M.K., Cayan, D.R., Riddle, L.G.: Variability of marine fog along the California coast, Scripps Institution
569 of Oceanography Report 95-2, 102 pp., 1995
570 Fritzke, B.: A growing neural gas network learns topologies, Adv. Neural Inf. Process. Syst. 7, 625–632, 1995
571 Gultepe, I., Milbrandt, J.A.: Microphysical observations and mesoscale model simulation of a warm fog case during
572 FRAM project, Pure Appl. Geophys 164, 1161-1178, doi:10.1007/978-3-7643-8419-7_4, 2007
573 Gultepe. I., Tardif, R., Michaelides, S.C., Cermak, I., Bott, A., Bendix, J., Müller, M.D., Pagowski, M., Hansen, B.,
574 Ellrod, G., Jacobs, W., Toth, S., Cober, S.G.: Fog research: a review of past achievements and future perspectives,
575 Pure and Appl. Geophys. 164(6-7), 1121-1159, doi:10.1007/s00024-007-0211-x, 2007
576 Hersbach, H.; Bell, B.; Berrisford, P.; Hirahara, S.; Horányi, A.; Muñoz-Sabater, J.; Nicolas, J.; Peubey, C.; Radu, R.;
577 Schepers, D.; Simmons, A.; Soci, C.; Abdalla, S.; Abellan, X.; Balsamo, G.; Bechtold, P.; Biavati, G.; Bidlot, J.;
578 Bonavita, M.; De Chiara, G.; Dahlgren, P.; Dee, D.; Diamantakis, M.; Dragani, R.; Flemming, J.; Forbes, R.; Fuentes,
579 M.; Geer, A.; Haimberger, L.; Healy, S.; Hogan, R. J.; Hólm, E.; Janisková, M.; Keeley, S.; Laloyaux, P.; Lopez, P.;
580 Lupu, C.; Radnoti, G.; de Rosnay, P.; Rozum, I.; Vamborg, F.; Villaume, S.; Thépaut, J.-N. (2020a): The ERA5 global
581 reanalysis, Q. J. R. Meteorol. Soc. 146, 1999–2049, doi:10.1002/qj.3803, 2020
582 Hersbach, H.; Bell, B.; Berrisford, P.; Hirahara, S.; Horányi, A.; Muñoz-Sabater, J.; Nicolas, J.; Peubey, C.; Radu, R.;
583 Schepers, D.; Simmons, A.; Soci, C.; Abdalla, S.; Abellan, X.; Balsamo, G.; Bechtold, P.; Biavati, G.; Bidlot, J.;
584 Bonavita, M.; De Chiara, G.; Dahlgren, P.; Dee, D.; Diamantakis, M.; Dragani, R.; Flemming, J.; Forbes, R.; Fuentes,
585 M.; Geer, A.; Haimberger, L.; Healy, S.; Hogan, R. J.; Hólm, E.; Janisková, M.; Keeley, S.; Laloyaux, P.; Lopez, P.;
586 Lupu, C.; Radnoti, G.; de Rosnay, P.; Rozum, I.; Vamborg, F.; Villaume, S.; Thépaut, J.-N. (2020b): ERA5 hourly
587 data on pressure levels from 1979 to present, Copernicus Climate Change Service (C3S) Climate Data Store (CDS),
588 doi:10.1002/qj.3803, 2020

589 Huang, B., Zhang, J., Cao, Y., Gao, X., Ma, S., Sun, C.: Improvements of sea fog forecasting based on CMA-TYM,
590 Front. Earth Sci. 10: 854438, doi: 10.1016/j.jastp.2022.105958, 2022
591 Ju, T., Wu, B., Zhang, H., Liu, J.: Parameterization of radiation fog-top height and methods evaluation in Tianjin,
592 Atmosphere 11(5), 480, doi:10.3390/atmos11050480, 2020
593 Kawai, H., Koshiro, T., Endo, H., Arakawa, O., Hagihara, Y., Changes in marine fog in a warmer climate., Atmos.
594 Sci. Lett. 17, 548-555, doi:10.1002/asl.691
595 Klaić Z. B., Pasarić Z., Tudor M.: On the interplay between sea-land breezes and etesian winds over the Adriatic, J.
596 Mar. Sys. 78, 101–118, doi: 10.1016/j.jmarsys.2009.01.016, 2009
597 Klemm, O., Lin, N.: What causes observed fog trends: air quality or climate change? Aerosol. Air. Qual. Res. 16,
598 1131-1142, doi:10.4209/aaqr.2015.05.0353
599 Koračin, D., and Dorman, C.E. (Eds): Marine fog: challenges and advancements in observations and forecasting,
600 Springer Atmospheric Sciences Series, Springer International Publishing, Cham, Switzerland, 537 pp.,
601 doi:10.1007/978-3-319-45229-6_7, ISBN 978-3-319-45227-2, 2017
602 Koračin, D., Lewis, J., Thompson, W.T., Dorman, C.E., Businger, J.A.: Transition of stratus into fog along the
603 California coast: observations and modeling, J. Atmos. Sci. 58, 1714-1731, doi:10.1175/1520-
604 0469(2001)058%3C1714:TOSIFA%3E2.0.CO;2, 2001
605 Kulkarni, R., Jenamani, R.K., Pithani, P., Konwar, M., Nigam, N., Ghude, S.D.: Loss to aviation economy due to
606 winter fog in New Delhi during the winter of 2011-2016, Atmosphere, 10(4), 198, doi:10.3390/atmos10040198, 2019
607 Li, G., Cheng, L., Zhu, J., Trenberth, K.: Increasing ocean stratification over the past half-century, Nat. Clim. Change
608 10(12), 1-8, doi:10.1038/s41558-020-00918-2, 2020
609 Mariani, L.: Fog in the Po valley: Some meteo-climatic aspects, Ital. J. Agrometeorol. 3: 35-44, 2009
610 Martinetz, T., Schulten, K.: A “neural-gas” network learns topologies, in: Proceedings of the International Conference
611 on Artificial Neural Networks 1991, 397-402, 1991
612 Matić, F., Džoić, T., Kalinić, H., Ćatipović, L., Udovičić, D., Juretić, T., Rakuljić, L., Sršen, D., Tičina, V.:
613 Observation of abrupt changes in the sea surface layer of the Adriatic Sea, J. Mar. Sci. Eng. 10, 848,
614 doi:10.3390/jmse10070848, 2022
615 Merchant, C. J.; Embury, O.; Bulgin, C. E.; Block, T.; Corlett, G. K.; Fiedler, E.; Good, S. A.; Mittaz, J.; Rayner, N.
616 A.; Berry, D.; Eastwood, S.; Taylor, M.; Tsushima, Y.; Waterfall, A.; Wilson, R.; Donlon, C.: Satellite-based time-
617 series of sea-surface temperature since 1981 for climate applications, Sci Data 6(1) 1-18, doi: 10.1038/s41597-019-
618 0236-x, 2019
619 Omazić, B., Telišman Prtenjak, M., Prša, I., Belušić Vozila, A., Vučetić, V., Karoglan, M., Karoglan Kontić, J., Prša,
620 Ž., Anić, M., Šimon, S., Güttler, I.: Climate change impacts on viticulture in Croatia; viticultural zoning and future
621 potential, Int. J. Climatol. 40, 5634 – 5655, doi:10.1002/joc.6541, 2020
622 Oztaner, Y.B., Yilmaz, A.: An examination of fog and PM10 Relationship for Ataturk and Esenboga International
623 Airports of Turkey, in: Proceedings of the 6th Atmospheric Science Symposium - ATMOS 2013, Istanbul Technical
624 University, 2013

Pandžić K., Likso T.: Eastern Adriatic typical wind field patterns and large-scale atmospheric conditions, Int. J. Climatol. 25, 81–98, doi:10.1002/joc.1085, 2005

Pastor, F., Valiente, J.A., Palau, J.L.: Sea surface temperature in the Mediterranean: trends and spatial patterns, Pure and Appl. Geophys. 175, 4017-4029, doi:10.1007/s00024-017-1739-z, 2018

Pawlowicz, R.: M_Map: A mapping package for MATLAB, version 1.4m, [Computer software], available online at www.eoas.ubc.ca/~rich/map.html, 2020

Popović, R., Kulović, M., Stanivuk, T.: Meteorological safety of entering eastern Adriatic ports, Trans. Marit. Sci. 2014 (1), 53-60, doi:10.7225/toms.v03.n01.006, 2014

Stipaničić, V.: Fog on the western coast of the Istria peninsula, Vijesti Pomorske meteorološke službe, 18, 7-10, https://library.foi.hr/dbook/cas.php?B=1&item=S02101&godina=1972&broj=00001, 1972

Stolaki, S.N., Kazadzis, S.A., Foris, D.V., Karacostas, Th.S.: Fog characteristics at the airport of Thessaloniki, Greece, Nat. Hazards Earth Syst. Sci. 9: 1541-1549, doi:10.5194/nhess-9-1541-2009, 2009

Šantić, D., Piwosz, K., Matić, F., Vrdoljak Tomaš, A., Arapov, J., Dean, J. L., Šolić, M., Koblížek, M., Kušpilić, G., Šestanović, S.: Artificial neural network analysis of microbial diversity in the central and southern Adriatic Sea, Sci. Rep. 11, 1–15, doi:10.1038/s41598-021-90863-7, 2021

Šimunić, I., Likso, T., Husnjak, S., Bubalo Kovačić, M.: Analysis of climate elements in central and western Istria for the purpose of determining irrigation requirements of agricultural crops, Agric. Conspec. Sci. 86(3), 225-233, https://hrcak.srce.hr/file/382381, 2021

Tardif, R., Rasmussen, R.M.: Event-based climatology and typology of fog in the New York City region, J, App. Meteorol. Climatol., 46, 1141-1168, doi:10.1175/JAM2516.1, 2007

Telišman Prtenjak, M., Grisogono, B.: Sea-land breeze climatological characteristics along the northern Croatian Adriatic coast, Theor. Appl. Climatol. 90, 201–215, doi:10.1007/s00704-006-0286-9, 2007

Telišman Prtenjak, M., Viher, M., Jurković, J.: Sea-land breeze development during a summer bora event along the north-eastern Adriatic coast, Q. J. Roy. Meteorol. Soc. 136, 1554–1571, doi:10.1002/qj.649, 2010

Tešić, M., Brozinčević, K.: Fog phenomenon on the eastern coast of the Adriatic Sea, Hidrografski godišnjak 1974, 91-116, 1974

Tojčić, I., Denamiel, C., Vilibić, I.: Kilometer-scale trends and variability of the Adriatic present climate, (1987–2017), Clim. Dyn 61, 2521–2545, 10.1007/s00382-023-06700-2

Tojčić, I., Denamiel, C., Vilibić, I.: Kilometer-scale trends, variability, and extremes of the Adriatic far-future climate (RCP 8.5, 2070-2100), Front. Mar. sci. 16, 907–926, doi:10.3389/fmars.2024.1329020, 2024

Vautard, R., Yiou, P., van Oldenborgh, G.: The decline of fog, mist and haze in Europe during the last 30 years, Nat. Geosci. 2, 115–119, doi:10.1038/ngeo414, 2009

Veljović, K., Vujović, D., Lazić, L.: An analysis of fog events at Belgrade International Airport, Theor. Appl. Climatol. 119 (1-2), 13-24, doi:10.1007/s00704-014-1090-6, 2015

WMO, International Meteorological Vocabulary, World Meteorological Organization, Geneva, Switzerland, pp. 141., 1966

Wang, Y., Niu, S. J., Lv, J. J., Lu, C. S., Xu, X. Q., Wang, Y. Y., Ding, J., Zhang, H., Wang, T., Kang, B.: A new method for distinguishing unactivated particles in cloud condensation nuclei measurements: implications for aerosol indirect effect evaluation, Geophys. Res. Lett. 46, 14185–14194, doi:10.1029/2019gl085379, 2019

Zoldoš, M., Jurković, J.: Fog event climatology for Zagreb Airport, Croatian Met. Journal 51(51), 13-26, https://hrcak.srce.hr/168218, 2016